17th World Conference on Earthquake Engineering, 17WCEE
Sendai, Japan - September 13th to 18th 2020

Experimental study on seismic behavior of RC beam-column joints considering axial restraint effects of beams

Wenwen Luo[(1)], Licheng Jiang[(2)], Shijian Yang [(3)], Liping Wang[(4)], Wei Zhang[(5)]

[(1)] *Lecturer, School of Civil Engineering and Architecture, Chongqing Univ. of Science and Technology, Chongqing 401331, China, luowenwen326@163.com*
[(2)] *Graduate Student, School of Civil Engineering and Architecture, Chongqing Univ. of Science and Technology, Chongqing 401331, China, 976701693@qq.com*
[(3)] *Graduate Student, School of Civil Engineering and Architecture, Chongqing Univ. of Science and Technology, Chongqing 401331, China, 815953755@qq.com*
[(4)] *Associate Professor, School of Civil Engineering and Architecture, Chongqing Univ. of Science and Technology, Chongqing 401331, wangliping98@163.com*
[(5)] *Graduate Student, School of Civil Engineering and Architecture, Chongqing Univ. of Science and Technology, Chongqing 401331, China, 632270766@qq.com*

Abstract

In the RC (reinforced concrete) frame structure, the axial elongation of the beam after flexural cracking and yielding is restrained by the surrounding structural components, resulting in a non-negligible axial constraint force in the beam. It will affect the seismic performance of the beam-column joints and the failure mode of structures under strong earthquake ground motions. This study aims at exploring the influence of the axial restraint effect of the beam on the seismic behavior of the beam-column joints. Experiments were conducted on two sets of four 1/2 interior beam-column subassemblies: one set was designed to meet the minimum requirements of ACI318-14 and Chinese seismic design provisions for the joint region; the other set was strengthened with the stirrup reinforcement for the joint region; both sets included two specimens with axial restrained and unrestrained condition, respectively. An equivalent restraint device was used to impose the restraint effect of the surrounding structural components on the beam end. The device was able to directly measure the axial constraint force of the beam. The shear resistance demand, shear capacity, and damage mode of the beam-column joints were studied through the cycle loading tests along with the theoretical analyses. The results suggested that the shear resistance demand and shear capacity of the beam-column joints both increased under the effects of the axial restraint force with beam elongation effects. However, the beam-column joints without axial restrained condition designed in accordance with the codes only had slight damage. In contrast, the joints under the axial restraint force suffered serious damage even if the stirrup ratio was doubled. Thus, the axial restraint force had more significant impact on the shear resistance demand of the beam-column joints than the shear capacity.

Keywords: reinforced concrete frame; axial restraint; beam elongation; beam-column joint.

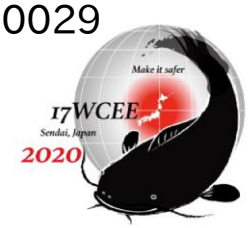

1. Introduction

The reasonable failure mechanism of RC frame buildings subjected to strong earthquakes is one of the key factors for achieving seismic fortification objectives. The seismic failure mechanism is designed based on capacity-ductility rule, following strong joint-weak member principles [1]. The beam-column joints play an important role in transferring and balancing internal force in the RC frame. If the joint is damaged under the earthquakes, it will have a great influence on the stiffness and deformation of the whole structure. However, even the capacity-ductility rule is adopted, the unexpected damage of RC beam-column joints frequently occurred in previous earthquakes [2, 3]. The insufficiency of joint stirrup ratio, concrete strength, and anchoring requirements of reinforced bars are usually explained as the main reason by previous researchers [4, 5]. However, the phenomenon of the axial elongation of the beam which is closely related to the shear performance of the joint is conventionally neglected.

RC beams tend to elongate after flexural cracking and yielding [6, 7]. It is resulted from geometric elongation, residual deformation of reinforced bars, contact stress effect and truss action effect in the plastic hinge regions of beams [6, 8]. However, beam elongation in a RC frame is restrained by the surrounding components such as cast-in place RC slabs and lateral force resisting systems. In turn, compressive axial force develops in the beam, thereby it affects the seismic performance of structure components and the whole structures [9-12]. Zerbe and Durrani [10] conducted cyclic lateral loading tests on a 1 story two-bay RC frame. Compressive axial force developed in the beam because the beam elongation was restrained by surrounding frame columns. The unexpected axial restrained force significantly increased the shear burden on beam-column joints, which resulted in more serious concrete damage and larger stirrup strain in the joint area. Kim et al. [13] analyzed the beam elongation effect by numerical simulations, which indicated that the beam axial force increased the shear requirement of joint. Previous research of the authors [14] revealed that under the considered levels of axial restraint, large compressive axial force was generated in the beams, leading to an axial force ratio up to 0.25. The influence of axial restrained force of this magnitude on the joint cannot be ignored. The compressive axial force substantially increases the shear demand of the joint, on the contrary, it also increases the shear resistant capacity of the joint by the restraint effect at the same time. However, the influence of compressive axial force in restrained beams on the mechanics performance and seismic performance of beam-column joints is not clear. Therefore, this paper presents a series of experiments to further examine the restraining effects on shear demand and performance in beam-column joints.

2. Shear in beam-column joint

Based on the capacity design principle of RC frame structure, the design value of joint shear demand is determined by the principle of strong joint-weak member, when the beam ends connected to both sides of the joint yield under positive and negative bending moments. If the axial force in the main beams is ignored, the equilibrium of forces acting on the joint is shown in Fig. 1(a). The shear demand of joint V_j is given in Eq. (1).

$$V_j = C_{s,l} + C_{c,l} + T_r - V_{c,u} = T_l + T_r - V_{c,u} \quad (1)$$

Where $C_{s,l}$, $C_{c,l}$ are compressive force of beam longitudinal bars and concrete at left beam-column interface, respectively. The T_r and T_l are severally tensile force of beam longitudinal bars at right and left beam-column interface, respectively. The $V_{c,u}$ indicates upper column shear force. The $C_{s,l} + C_{c,l}$ developed by beam flexural yielding are equivalent to T_l.

However, if the compressive axial force in restrained beam is present, it would transfer from the compressive region of beam on one side of the joint to the other side, as shown in Fig.1(b). The shear demand of joint V_j is determined by Eq. (2).

$$V_j = C_{s,l} + N_{s,l} + C_{c,l} + N_{c,l} + T_r - V_{c,u} = T_l + T_r + N_l - V_{c,u} \quad (2)$$

Where $N_{s,l}$, $N_{c,l}$ are the axial force of beam longitudinal bars and concrete at left beam-column interface, respectively. The N_l is the total of axial force at left beam-column interface transferring into the joint regions.

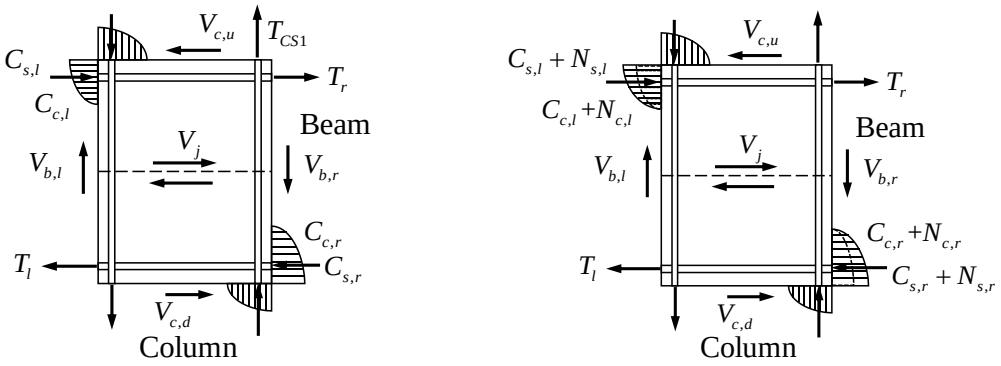

(a) Excluding Beam Axial force (b) Including Beam Axial force

Fig.1 - Internal Stress Resultant in Beam-Column Joint.

When beam ends suffer a flexural yielding, the tensile force of longitudinal reinforcements T_l and T_r keeps constant. Beam flexural capacity is enhanced by the compressive axial force. And according to the moment equilibrium at the joint, the shear force of column $V_{c,u}$ increases as the moment of column increases. Additionally, a part of axial force in the beam directly transfer into column from the compressive region of beam ends informed the column shear force. With the compressive axial force in restrained beam, the shear demand primarily depends on the relative variation $N_l - V_{c,u}$ of restraint force N_l and column shear force $V_{c,u}$. At the same time, the shear resistant capacity of joint would be increased by the beam axial restraint effect. To reveal the influence of the axial force on the shear demand and seismic performance of joint, this paper presents the results of an experimental investigation in which the behavior of joint was studied under cyclic lateral loading by testing beam-column subassemblies.

3. Test Setup and Properties

3.1 Design of Specimens and Test Setup

Four specimens constructed at a 1/2 scale were tested. The specimens represented the interior beam-column subassemblies of a multibay, multistory RC frame prototype building with an 8-m span length and a 3.2-m story height. The transverse reinforcement ratio of joint and the axial restraint level were considered as test variables. Four specimens, namely 3NS, 3HS, 3N and 3H, are listed in Table 1. Specimens 3NS and 3HS were designed and detailed based on the minimum requirements of ACI318-14 [15] and the Chinese seismic design code [16] for transverse reinforcement of joint. Specimens 3N and 3H were strengthened with transverse reinforcement of joint to avoid joint failure, which were chosen from previous experiments [14]. The letters N and H indicate restraining rigidity levels corresponding to zero and high restraining stiffness, respectively. Fig.2 shows the test setup. The axial restraint system is shown in Fig.3, which simulated the passively generated axial force that varies along with increasing plastic deformation of the RC frame beam. When beam elongation restrained by the steel rods, the compressive axial force in beam and the tensile axial force in steel rods that measured by the compressive cells located at steel rods were equivalent in value. Steel rods with a diameter of 60 mm were used to achieve the axial restraining rigidity that may be encountered in

a RC frame (after scaling). Details could be obtained from reference [14]. As column compressive axial force is conducive to the shear resistance of joint, no axial load was applied to the column during lateral loading.

Fig.2 - Test setup of 3NS and 3HS.

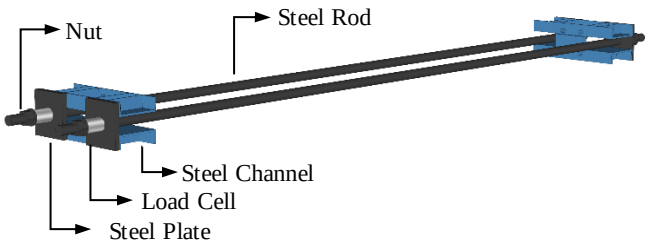

Fig.3 - Axial restraint system.

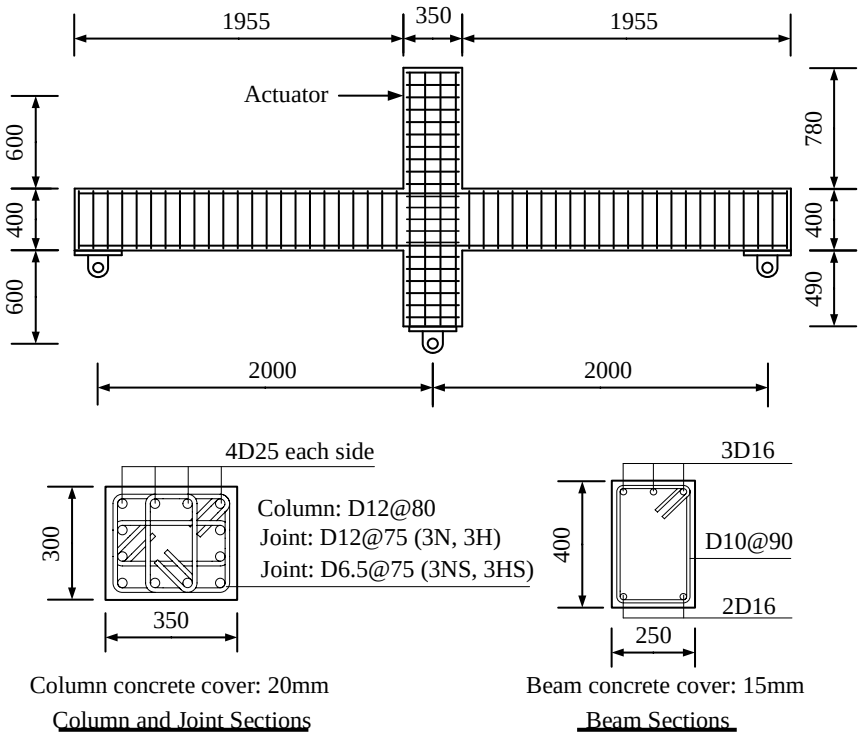

Fig.4 - Dimensions (in millimeters) and reinforcing details of test specimens.

Fig.4 and Table 1 shows specimens dimensions and reinforcing details. The effective longitudinal dimension of a specimen was 4 m. The effective column height was 1.6 m. Each beam had a width of 250 mm and height of 400 mm. The column cross-sectional dimension was 350 mm in the loading direction and 300 mm in the transverse direction. The longitudinal reinforcement had a 16-mm (D16) diameter for the beams and 25-mm (D25) diameter for the columns. Because the experiments focused on the performance of beams and beam-column joints, each column was heavily reinforced. Rectangular hoops made of D10 bars were used as beam transverse reinforcement and were uniformly distributed at a center-to-center spacing of 90 mm. The transverse reinforcement of the columns contained two overlapping D12 hoops with a spacing of 80 mm. The beam-column joint contained two overlapping D12 hoops with a spacing of 75 mm for Specimens 3N and 3H, two overlapping D6.5 hoops with a spacing of 75 mm for Specimens 3NS and 3HS. All reinforcement was deformed bars. The clear concrete cover was specified as 15 mm for the beams and 20

mm for the columns. Table 1 gives the yield strengths of the reinforcing bars and the cylinder compressive strength of concrete measured after the completion of an experiment.

Table 1 - Test specimens, material properties, and axial restraining rigidity

Specimen	Yield strength of reinforcing bars (MPa)					Concrete strength (MPa)	Joint transverse reinforcement	Axial restraining steel rod diameter (mm)
	D25	D16	D12	D10	D6.5			
3NS	493	471	614	673	428	39.9	6.5@75	-
3HS	493	471	614	673	428	38.0	6.5@75	60
3N	473	493	545	595	-	28.7	12@75	-
3H	473	471	545	595	-	31.9	12@75	60

3.2 Loading Protocol and Instrumentation

A displacement-controlled lateral loading was applied to the column top using a 500-kN capacity hydraulic actuator. Fig.5 shows the cyclic lateral loading history, each specimen had eight drift levels including 0.375%, 0.5%, 0.75%, 1%, 1.5%, 2%, 3% and 4% with three cycles at each drift level. Lateral pushing was defined as positive signs, and lateral pulling was defined as negative signs.

The lateral loading was applied by the actuator and the vertical reaction force at beam ends was measured by tensile or compressive force cells. LVDTs were used to measure the horizontal displacements at the column top, and beam ends. Based on the measured beam horizontal movements at various locations, the overall beam elongation was determined.

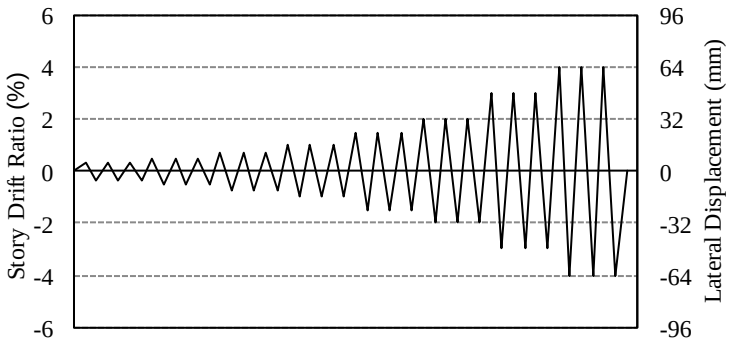

Fig.5 - Cyclic lateral loading history.

4. Experiment Results

4.1 Beam elongation and axial force

Fig. 6 compares the beam elongation history of the unrestrained Specimen (3NS and 3N) and the restrained Specimen (3HS and 3H). Prior to 1% drift, the beams behaved in elastic manner, and the cracks were narrow and closed almost completely upon unloading. Accordingly, the beam elongation was low and recoverable. At 2% drift, the beam elongations of the Specimen 3NS and 3N were about 8.70 mm and 8.43 mm, respectively. Corresponding, the residual beam elongations were 6.99 mm and 6.58 mm, respectively. At 4% drift, the elongations of 3NS and 3N were as high as 14.72 mm and 18.02mm, respectively. And the residual

beam elongations were 12.70 mm and 15.74 mm, respectively. Without axial restraint, the beam could elongate freely after flexural cracking and yielding, and the free elongation could reach centimeter level. In contrast, when the axial restraint existed, the beam elongation would be restrained obviously. At 2% drift, the beam elongations of Specimen 3HS and 3H were about 3.60mm and 4.97mm, and the residual beam elongations were 1.21 mm and 2.43 mm, respectively. At 4% drift, the elongations of Specimens 3HS and 3H were about 4.77mm and 7.20mm, and the corresponding residual beam elongations were 2.43mm and 3.43mm, respectively.

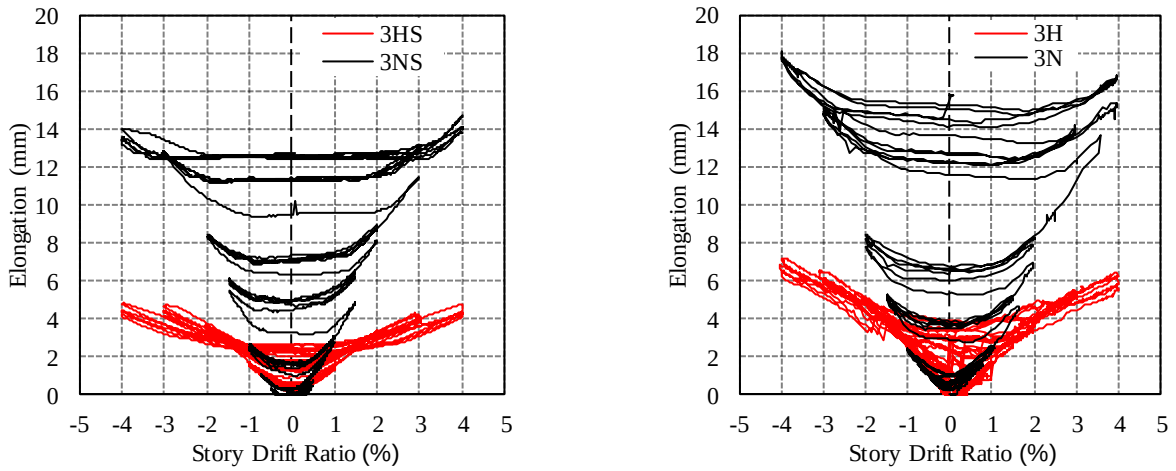

Fig.6 - Beam elongation history

As shown in Fig.7, for Specimens 3HS and 3H, a large compressive axial force was generated in the restrained beams during lateral loading. Prior to 1% drift, the axial force diminished upon unloading because beam elongation was caused primarily by the geometric elongation which could restored when unloading. At a drift beyond 1%, the axial force gradually increased. At 4% drift, the beam axial force was about 750kN and 800kN, respectively. Because of the different concrete strengths of the specimens, the passively developed beam axial force was normalized into axial force ratio. The ratio ranged between 0.10-0.14 at 2% drift and 0.16-0.19 at 4% for Specimen 3HS. For Specimen 3H, the ratio ranged between 0.13-0.17 at 2% drift and 0.2-0.25 at 4% drift.

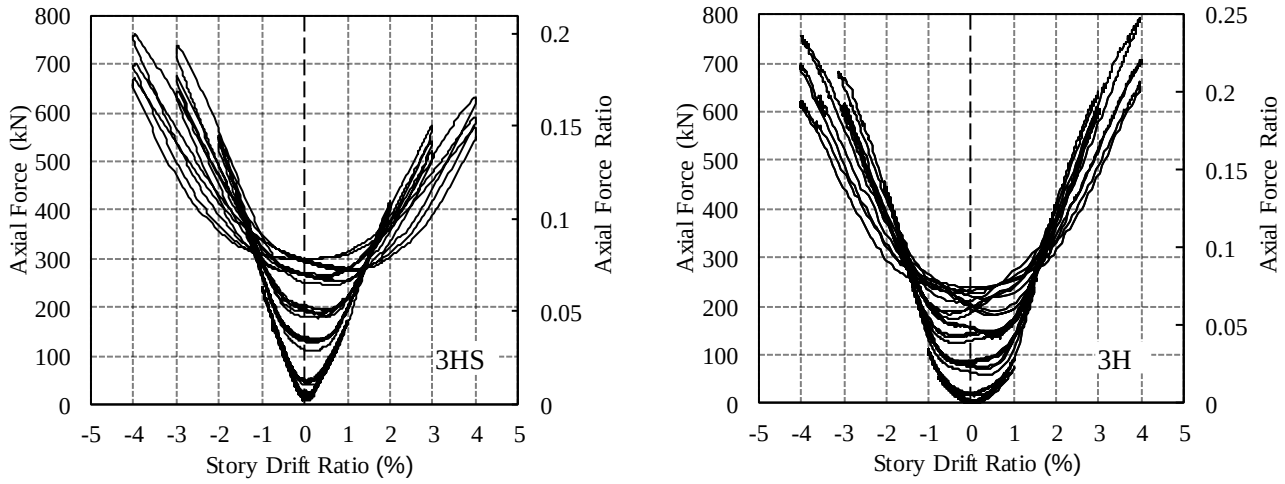

Fig.7 - Beam axial force and axial force ratio.

4.2 Hysteretic Response

Fig. 8 shows the hysteretic response of lateral load versus drift for the test specimens. The unrestrained Specimens 3NS and 3N presented a yield plateau in their response envelopes. And the hysteretic hoops for unrestraint Specimens 3NS and 3N had an obvious pinching effect indicating the longitudinal reinforcement developed a large bond slip in plastic hinges regions of beam and joint regions. The restrained Specimens 3HS and 3H, which had similar concrete strength and transverse reinforcement ratio of joint to that of their unrestrained counterparts (3NS and 3N), showed a reduced degree of pinching. Except for Specimen 3HS, the other specimens did not experience strength degradation by the completion of 4% drift. Specimen 3HS experienced evidently strength degradation between 3% drift and 4% drift. Compared with Specimen 3H, the pinching effect of 3HS was more significant, which indicate that the shear deformation in the joint of 3HS was larger than that in 3H. Additionally, as described subsequently, the axial restraining force kept increasing as lateral drift increased. As a result, the flexural capacity of beams was enhanced through axial force-flexure interaction. As such, the restrained specimens did not present a yield plateau in the response envelop. At 2% drift, with axial restraint, the lateral load of the Specimen 3HS and 3H were 225kN and 211kN, 1.83 and 1.80 times that of the Specimen 3NS and 3N, respectively. At 4% drift, the lateral load of Specimen 3HS and 3H were 224kN and 269kN, 1.96 and 2.42 times that of the Specimen 3NS and 3N, respectively. Such a strength increase may remarkably alter the upper column shear requirement, which indirectly affects the shear requirement of the joint V_j .

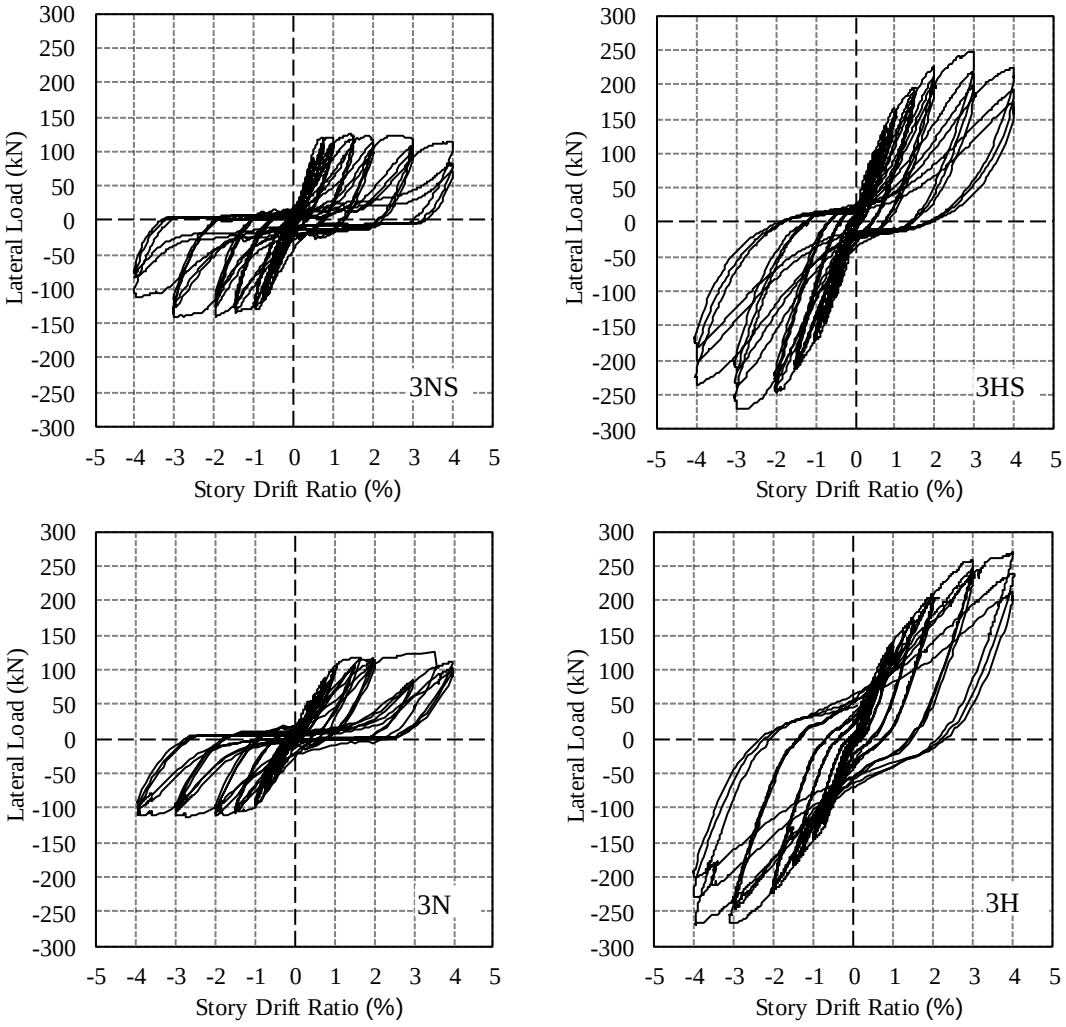

Fig.8 - Hysteretic response of lateral load versus drift.

4.3 Shear demand in joint

With axial restraint effects, the flexural capacity of the specimens was enhanced by the large compressive axial forces in the beam, and the shear force of upper column was also increased. The shear demand of joint was caculated using Eq.(1) and Eq.(2). The measured strains of beam upper longitudinal reforcing bars indicated that the flexural yielding of the beam occurred between 0.6% drift and 1.3% drift. To calculate T_l and T_r, the tensile stress of reinforcing bars was assumed as 1.25 times of the yield strength at 1.5% and higher drift ratios to account for possible strain hardening per ACI 318-14 [15]. N_l and $V_{c,u}$ could be obtained from the compressive load cells in the axial restraint system and load cells in the actuator. The shear force demand of joint at 1.5%, 2%, 3%, 4% drift was listed in Table 2.

Table 2 - Shear demand of joint

Specimen	Drift ratio (%)							
	+1.5	-1.5	+2	-2	+3	-3	+4	-4
3NS	466	458	468	452	468	450	477	480
3HS	696	789	780	892	906	1037	997	1118
3N	503	514	503	510	494	507	508	509
3H	655	684	790	823	968	996	1116	1078

The shear demand V_j is depend on the relative change of $N_l - V_{c,u}$, as shown by the opposite signs of N_l and $V_{c,u}$ in Eq. (2). At 2% drift, the shear demand of Specimen 3HS and 3H were 780kN and 790kN, about 1.66 and 1.57 times that of Specimen 3NS and 3N, respectively. At 4% drift, the shear demand of Specimen 3HS and 3H were 997kN and 1116kN, about 2.09 and 2.2 times that of Specimen 3NS and 3N, respectively. The compressive axial force N_l generated in the beam considering axial restraint effect dramatically increased the shear demand in the beam-column joint.

The effect of beam axial force is twofold. On one hand, it dramatically increased the shear demand of joint. On the other hand, it also increased the shear resistance capacity of joint due to considering the restraint effect. It is similar to the effect of the prestressed action of beam passing through the joint on shear resistance of beam-column joints in prestressed concrete frame. To preliminarily consider this beneficial effect, the shear resistance capacity V_c of Specimen 3HS and 3H defined by JGJ 140-2004 [17] was shown in Eq.(3). The N_{pe} of Eq.(3) herein is considered as beam axial force. For Specimen 3NS and 3N, the beam axial force N_{pe} is ignored.

$$V_c = 1.1\eta_j f_t b_j h_j + 0.05\eta_j N\left(b_j / b_c\right) + f_{yv}\left(A_{svj}/s\right)\left(h_{b0} - a_s^{'}\right) + 0.4N_{pe} \tag{3}$$

Where η_j is the confined effect factor of the orthogonal beams, herein $\eta_j = 1.0$; f_t is concrete axial tensile strength; b_j is the effective width of the cross section at the zone of the joint, herein $b_j = 300\text{mm}$; h_j is cross-sectional height at the core zone of the joint, herein $h_j = 350\text{mm}$; N is the axial compressive force of the upper column, herein $N=0$; b_c is the width of column cross-sectiom, herein $b_c = 300\text{mm}$; f_{yv} is yield strength of stirrup; A_{svj} is total stirrup cross-sectional area within the same cross section in the effective width of the core zone; s is the spacing of stirrup; h_{b0} is the effective depth of the beam section, herein $h_{b0} = 367\text{mm}$; $\alpha_s^{'}$ is the distance measured from the extreme compression fiber to compressive

reinforcement of the beam, $\alpha_s^{'} = 33\text{mm}$; N_{pe} is the effective prestress force acting on the joint core, herein it is considered as beam axial force.

A shear demand ratio equal to V_j/V_c was evaluated based on the test data for each specimen at 1.5%, 2%, 3%, and 4% drift, shown in Fig.9. The shear demand ratio of Specimen 3NS and 3N was about 0.84 and 0.36, and kept steadily for the whole test process. On the contrary, the shear demand ratio of axial restraint Specimen 3HS and 3H, increased approximately linearly. For Specimen 3H designed with enough redundant joint shear resistance, the shear demand ratio increased from about 0.44 to 0.66, and less than 1.0. For axial restrained Specimen 3HS, the transverse reinforcement of joint was designed and detailed based on the minimum requirements of ACI318-14 and Chinese seismic design provisions. The shear demand ratio of Specimen 3HS increased from 1.02 at 1.5% drift to 1.22 at 4% drift. Compared with the unrestrained Specimen 3NS, the shear demand ratio of Specimen 3HS increased 1.41 times at 2% drift, and 1.50 times at 4% drift, respectively. The remarkable increase in shear demand ratio explained the noticeable damage to the joint of Specimen 3HS, described thereafter, and can significantly reduce the strength margin of beam-column joint.

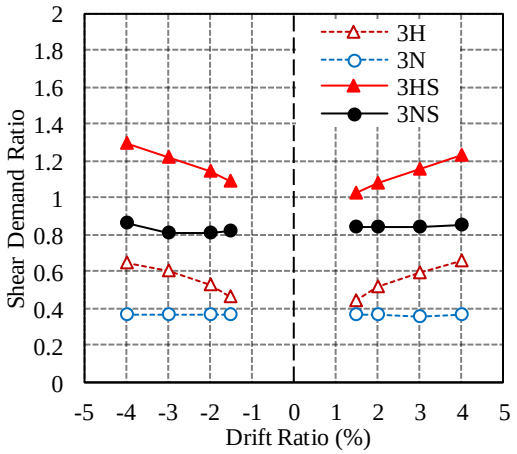

Fig.9 - Shear demand ratio of joint.

4.4 Damage Patterns in Beam-Column Joints

Figs.10 and 11 show the damage patterns in plastic hinge and beam-column joint regions of four specimens at 2.0% and 4.0% drifts. The performance of the unrestrained Specimen 3NS and 3N was dominated by flexural behavior, and the lateral drift beyond beam yielding was accommodated mainly by bond slip in the beam plastic hinge regions and the joint. Beam flexural cracking occurred at the first drift level of 0.375% drift. By 2% drift, the flexural cracks at the beam-column interface became much wider than 2 mm, penetrated the entire beam depth, and could not be completely closed in the subsequent loading reversals. Very few new cracks were further developed in the joints of Specimen 3N and 3NS at a drift beyond 2% drift. Damage to the beams due to spalling of concrete cover occurred at 3% drift in 3N, but it was limited within small regions. The damage pattern of Specimen 3NS whose transverse reinforcement was designed and detailed based on the minimum requirements of ACI318-14 and Chinese seismic design provisions, was almost identical to Specimen 3N.

The axial restraint effect of Specimen 3HS and 3H significantly affected the extent of damage. The existence of compressive axial force delayed the opening of beam flexural cracks. For Specimen 3HS and 3H, similar to the unrestrained specimens, crushing of beam concrete in the restrained specimens did not occur until 3% drift. However, as shown in Fig. 11, damage to the beam plastic hinge regions was remarkably more severe at 4% drift.

Damage to the beam-column joints was also more severe in the restrained specimens. Diagonal shear cracks appeared in the joint of each specimen by 0.5% drift. The Specimen 3H was designed with enough

redundant joint shear resistance, the damage of joint region is not as serious as that of specimen 3HS. The Specimen 3HS experienced severe strength degradation between 3% and 4% drift, as shown in Fig. 8. And the pinching effect of Specimen 3HS was more serious than that of Specimen 3H. The beam-column joint of Specimen 3HS suffered severe damage.

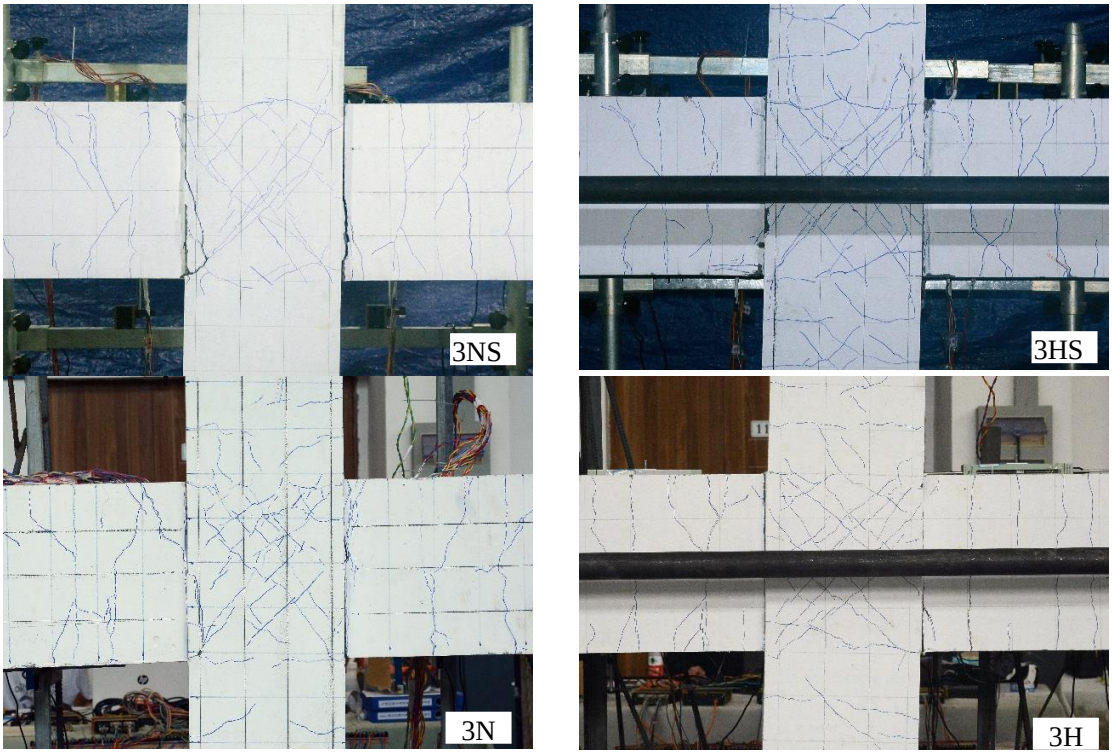

Fig.10 - Damage condition of specimens at 2% lateral drift.

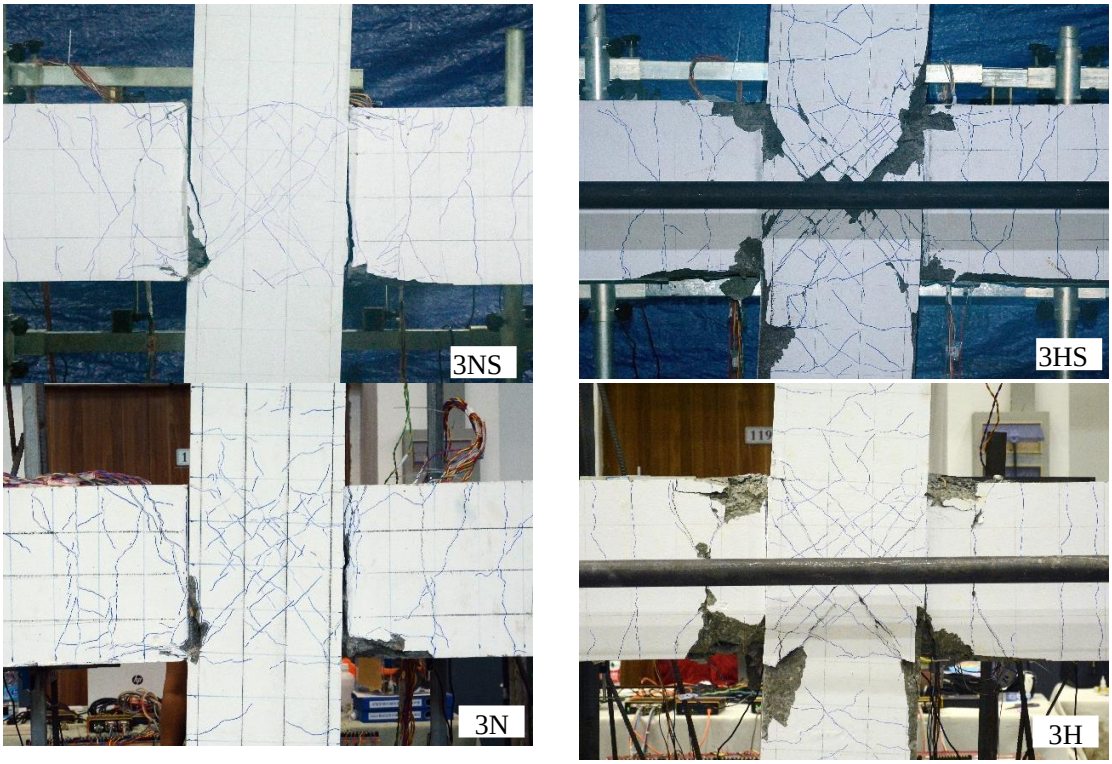

Fig.11 - Damage condition of specimens at 4% lateral drift.

5. Conclusions

Four specimens constructed at 1/2 scale were tested to examine the effects of axial restraints on the shear demand and seismic performance of joints. The following observations and preliminary conclusions were made from the tests:

(1) Without appliying axial restraints, the seismic performance of the beam-column subassembly was dominated by flexure behavior, and the lateral drift beyond beam yielding was accommodated mainly by bond slip in the beam plastic hinge regions and joints. Large beam elongation was developed after beam flexural cracking and yielding, and the unrestrained beams elongated about 2.0% of its height at 2% drift and 4.0% of its height at 4% drift.

(2) At the considered levels of axial restraints, the beam elongation was restrained to about 1% of the beam height at 2% drift and 1.8% of the beam height at 4.0% drift. And a large compressive axial force was generated in the beams, leading to an axial force ratio up to 0.25. The axial restraint increased flexural strength of the beams.

(3) Beam axial restraint can considerably increase shear demand in beam-column joints. However, the shear resistance of beam-column joint was aslo improved by the beam axial restraint effect. Overall, the beam axial restraint effect seem an unfavorable factor in seismic performance of beam-column joint. Compared with the unrestrained specimens, the ratio of shear demand to capacity defined by Chinese seismic design provisions increased about 1.5 times for the restrained specimens. Accordingly, the beam-column joint suffered severe damage.

6. Acknowledgements

The authors are grateful for the financial supports received from the National Natural Science Foundation of China (No. 51808087) and Chongqing Science and Technology Commission (cstc2018jcyjAX0695 and cstc2018jcyjAX0052). The authors also gratefully acknowledge Prof. Tian Ying from Univ. of Nevada for his valuable advice to experimental design and result analysis.

7. Copyrights

8. References

[1] Dooley KL, Bracci JM (2001): Seismic evaluation of column-to-beam strength ratios in reinforced concrete frames. *ACI Structural Journal*, 98(6): 843-851.

[2] Ye L, Qu Z, Ma Q et al (2008): Study on ensuring the strong column-weak beam mechanism for RC frames based on the damage analysis in the Wenchuan earthquake. *Building Structure*, 38(11): 52-59.

[3] Wang W Xue J, Zhang H, et al (2009): Seismic design and lessons learnt from the earthquake disaster of frame structures in 5.12 Wenchuan earthquake. *World Earthquake Engineering*, 25(4): 131-135.

[4] Tian Z, Zhang X, Zhao T (2009). Seismic damage of multilayer reinforced concrete frame structures in Wenchuan Earthquake. *Building Structure*, 39(11): 67-71.

[5] Zhou W, Zheng W, Tong J, et al (2013): Seismic strengthening and damage analysis of buildings in Wenchuan earthquake. *Journal of harbin institute of technology*, 45(12): 1-9.

[6] Fenwick RC, Megget LM (1993): Elongation and load deflection characteristics of reinforced concrete members containing plastic hinges. *Bulletin of the New Zealand National Society for Earthquake Engineering*, 26(1): 28-41.

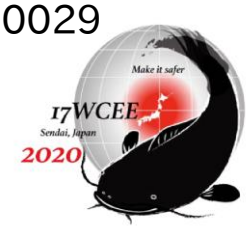

[7] Ashtiani MS, Dhakal RP, Scott AN (2014): Seismic Performance of High-Strength Self-Compacting Concrete in Reinforced Concrete Beam-Column Joints. *Journal of Structural Engineering*, 140(5): 401-402.

[8] Encina E, Lu Y, Henry RS (2016): Axial elongation in ductile reinforced concrete walls. *Bulletin of the New Zealand Society for Earthquake Engineering*, 49(4):305-318.

[9] Kokusho S, Hayashi S, Wada A, et al (1988): Behaviors of reinforced concrete beam subjected to the axial restriction of deformation. *Proceedings of Ninth World Conference on Earthquake Engineering*, Tokyo-Kyoto, Japan, 1988.

[10] Zerbe HE, Durrani AJ (1989): Seismic Response of Connections in Two-Bay RC Frame Subassemblies. *Journal of Structural Engineering*, 115(11): 2829-2844.

[11] Sakata H, Wada A (1992): Elasto-plastic behavior of one-twentieth scale RC frame. *Proceedings of Tenth World Conference on Earthquake Engineering*, Balkema, Rotterdam.

[12] Maeda M, Kabeyasawa T, Sanada Y (1999): Test and analysis of reinforced concrete beams under axial restraint. *U.S.-Japan Workshop on Performance-Based Earthquake Engineering Methodology for Reinforced Concrete Building Structures*, Maui, Hawaii.

[13] Kim J, Stanton J, Macrae G (2004): Effect of beam growth on reinforced concrete frames. *Journal of Structural Engineering*, 130(9): 1333-1342.

[14] Wang L, Tian Y, Luo W, et al (2019): Seismic Performance of Axially Restrained Reinforced Concrete Frame Beams. *Journal of Structural Engineering*, 145(5): 4019019.

[15] ACI (American Concrete Institute) (2014): Building code requirements for structural concrete. *ACI 318*, Detroit: ACI..

[16] CMC (China Ministry of Construction) (2010): Code for seismic design of buildings. *GB 50011*, Beijing: CMC.

[17] CMC (China Ministry of Construction) (2004): Specification for seismic design of prestressed concrete structures. *JGJ140*, Beijing: CMC.

